11th International Conference on Through-life Engineering Services – TESConf2022
8-9 November 2022, Cranfield UK

A practical demonstration of autonomous ultrasonic testing for rail flaws inspection

Feiyang He[a], Isidro Durazo-Cardenas[a,*], Haochen Liu[a], Miftahur Rahman[a], Masoumeh Rahimi[a], Andrew Starr[a], Michael Poulter[b]

[a]*Centre for Life-Cycle Engineering and Management, Cranfield University, Cranfield, MK43 0AL, United Kingdom*

[b]*Network Rail, Milton Keynes, MK9 1EN, United Kingdom*

* Corresponding author. Tel.: +44 (0) 1234 750111. *E-mail address:* i.s.durazocardenas@cranfield.ac.uk

Abstract

This study established the viability of autonomous ultrasonic inspections at the technology readiness level 5 (TRL 5). An autonomous ultrasonic rail inspection prototype was developed using commercially available ultrasonic instruments and an unmanned on-track vehicle platform consisting of a Clearpath's Warthog and a road-rail vehicle (RRV) trolley. The prototype was designed to travel back and forth on a segment of the test track during the test programme. Repeated fault checks were able to discover seeded artificial flaws at depths of 23 and 27 mm. The detection was indicated by an audio alarm triggered when the ultrasonic emissions exceeded the threshold of the detector gate. A plain text message sent over local area network (LAN) WIFI to a virtual server was also used to demonstrate the transmission of detection messages. The repeatability of the inspection prototype's positioning relative to the problem was confirmed using odometry, global navigation satellite system (GNSS), and positional measurements. The results of the three measurement methods were in good agreement, and the positioning inaccuracy varied between 3 and 7 cm. This study demonstrated the potential of autonomous ultrasonic checks and gave recommendations for further work and limitations.

Keywords: Autonomous; Ultrasonic; Rail; Inspection

1. Introduction

Economic growth is significantly facilitated by railway infrastructure. The number of train travels in the United Kingdom has climbed by 89 percent over the last two decades, reaching a new high of 1,8 billion in 2018-19 [1] Clearly, timely rail inspection and maintenance work are crucial to avoid catastrophic failure due to the track flaws caused by rising demands. Non-destructive testing (NDT) techniques are widely employed as preventative measures against track failures and potential derailment. Among these, ultrasonic railway testing (UT) is one of the most common and routine methods [2].

UT involves sending an ultrasonic beam into a rail using a probe. A transducer receives reflected echo signals from an interface, such as the back of an item or an imperfection. The severity and depth are interpreted using the intensity and arrival time of the reflection. Network Rail's ultrasonic testing unit (UTU) fleet is one of the most effective technologies for ultrasonic inspections of plain line tracks. Since their implementation, regular line inspections have substantially decreased the frequency of yearly train breakdowns. Nevertheless, pedestrian inspections are still necessary to handle localised faults and check the severity of UTU-identified indicators. These inspections may be expensive, labour-intensive, and almost often include safety concerns for pedestrian access. Autonomous rail inspection and repair systems (RIRS) may mitigate these problems [3].

Based in literature sources, the autonomy level of RIRS could be classified as Level 4 Human supervised based on [4] or Level 3 based on [5].[4]–[6]RIRS concept commands vehicles that can navigate itself on the track to the specified location, complete the ultrasonic inspection task, provide feedback on the inspection results and return to the starting point automatically. [4][5]

Several studies [7]–[11] have suggested using an unmanned aerial vehicle (UAV) and image recognition algorithms to identify rail faults autonomously, using recognition and tracking based on computer vision. They are limited to guiding the UAV flying along the track rail rather than conducting autonomous flaw inspection tasks [7]–[9]. On the other hand, [10] proposed UAV-based autonomous aerial photogrammetry to replace a bi-annually traditional survey inspection method for the rail tracks in an Automated Container Terminal. The study developed and evaluated several intelligent mission planning algorithms for drones in a simulation environment to reduce flight time. The optimised method was implemented in a control station's Android tablet app and verified in practice.

And in another study that comes closest to practical application, Aydin et al. proposed a method to detect the rail flaws by semantic segmentation from the rail images obtained by an autonomous UAV [11].

However, the studies using drones mentioned above could only capture images of the surface of the rail tracks, and their capacity to identify subsurface flaws is severely restricted. Therefore, other researchers have suggested autonomous, instrumented carts with UT-based inspection capabilities. However, they were in the first phases of technological advancement [12], [13].

This research aims to provide reliable and consistent fault inspection capabilities along an extended piece of the test track. The objectives include the development of a test prototype for autonomous ultrasonic testing on TRL 5, which represents that this technology is validated in a realistic environment. This research was not intended to produce new inspection and repair procedures. And instead, it utilised both off-the-shelf equipment and components as well as the most recent technological advances in autonomous research.

The scope limitations of the research were defined as follows:

In scope:

• To demonstrate inspections utilising an available autonomous vehicle and road-rail vehicle (RRV) conversion on a plain test track.

Out of scope:

• Development of new UT technology because it is already a mature application.

• Rail flaws repairing

• Switches & Crossings were not subject to demonstrations.

• Fully autonomous flaw assessment and detection in practical applications because of the TRL5 limitation.

2. Methodology

2.1. Inspection prototype development

The research designed an inspection prototype consisting of a UT, an autonomous vehicle and an RRV vehicle conversion, as shown in Figure 1. This section describes each of these components and the final prototype in detail.

2.1.1. Ultrasonic probe and flaw detector

This prototype utilised the Rail Scan 125 by Sonatest, a rail-established UT system, as shown in Figure 2. The rail walking stick is capable of manually inspecting and sizing rail defects and measuring rail bottom depth. The UT system's probe frequency is 2.5 MHz, with adjustable beam inspection settings of 0, 70 and 0-70 degrees.

Fig. 1. Inspection prototype.

The UT probe/flaw detector was calibrated prior to testing. The construction of a 1.4-meter-long calibration rail is depicted in Figure 3. The calibration rail simulated two sets of flaws. In the first set, two holes with an 8mm diameter were drilled at depths of 23 and 27 mm through the rail head. A second simulated defect comprising a 7.5mm diameter flat bottomed hole was machined at an angle of 70° and a depth of 50 mm from the rail end.

Fig. 2. Rail walking stick, probe and flaw detector of UT system.

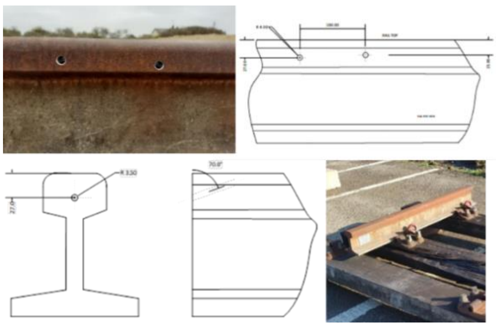

Fig. 3. Calibration rail.

During calibration, the flaw detector was calibrated to the simulated rail defects' size, location, and depth. The fault signatures in terms of signal amplitude and depth were recorded, and "Gate1" was configured accordingly. The Gain settings were also adjusted to better identify the peak associated with the artificial flaws.

2.1.2. Autonomous vehicle and RRV trolley

An all-terrain unmanned ground vehicle (UGV) Warthog, manufactured by ClearPath Robotics, was utilised as the drive unit in the test (Figure 4). It was suitable for the real challenging rail inspection environment. Furthermore, the vehicle was equipped with real-time kinematics (RTK)-enhanced Global navigation satellite system (GNSS). It can locate vehicles and rail defects with an accuracy of up to 3 cm. The vehicle was also compatible with ROS software. Therefore, it supported the integration, programming and modelling of the automation processes required to perform inspection and repair tasks. Finally, Warthog achieved level 4-automated based on UGV autonomy levels guideline [6].

Fig. 4. ClearPath's Warthog unmanned ground vehicle.

Because the width of the Warthog vehicle wheelset was narrower than that of the British railway's gauge, an RRV platform was necessary for on-track testing. Therefore, a trolley was designed and constructed, as shown in Figure 5.

Fig. 5. RRV conversion trolley.

2.1.3. Prototype assembly and communication development

The UT system was fixed to the front of the trolley by a bracket. The Warthog vehicle was loaded on the trolly.

A simple electronic circuit, constructed with commercially available components such as Arduinos, a modem, and a few other micro-components, emulated communications between the prototype and the command-and-control base.

Figure 6 depicts the communication method's operating concept. It utilises the Railscan 125 flaw detector's 14v output. This output is only triggered when the ultrasonic signal exceeds the Gate threshold on flaw detection. After passing via a voltage divider, the voltage is decreased from 14 to 5 VDC for input to an Arduino via cable. The Arduino is programmed to respond by sending a basic text code to a high-powered WIFI router that reads "flaw detected." The router then transmits the message to a base's command and control server, simulated by a tablet in the demonstration. At this stage, any further data from the Warthog vehicle, such as GPS locations, can be integrated with the first notification of fault detection. The Arduino, Warthog and tablet are connected to the router's wireless Local Area Network (LAN). Therefore, communication speed is guaranteed throughout the system, and there is no significant signal latency.

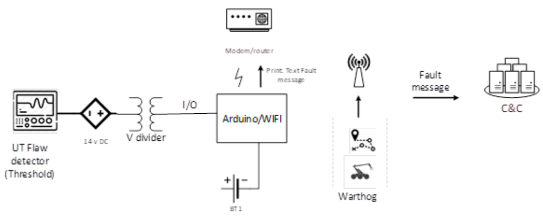

Fig. 6. Schematic for flaw detection communications to base.

2.2. Experimental procedures

Tests were undertaken at Cranfield's Rail and Innovation Test Area using a disused 18 m Vignole track panel representing a realistic environment (TRL5). A 1.4 m extended rail panel sample with simulated machined defects was attached at one end of the 18 m test track. The tests aimed to assess the prototype’s autonomous capabilities, system integration performance, communication functionality and localisation accuracy. The success of the inspection tests was defined as a function of repeated successful GPS-tagged flaw detections, which could confirm this integrated system's automation and communication performance.

Three on-track tests were designed and completed to verify the repeatability of the autonomous ultrasonic examinations. In each of these tests, the inspection prototype was programmed to navigate 5 m back-and-forth along the test track in both directions, as shown in Figure 7. The initial reference datum position was where the ultrasonic inspection equipment detected the simulated faults. The prototype positional error was defined as the distance between the datum reference and the end location of the inspection probe after each test. This was determined by three methods:

GNSS RTK enhanced signal, odometry and physical measurements of the starting and returning positions using markers, as shown in Figure 8. The latter method was used because the prototype GNSS navigation capability had not been tested before nor integrated with an operator graphical user interface (GUI). Therefore, the marker measurements mitigated these uncertainties and, at the same time, provided navigation verification.

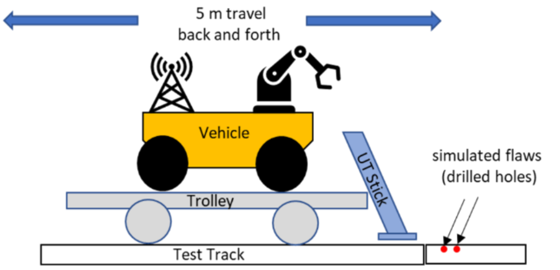

Fig. 7. Test set illustration.

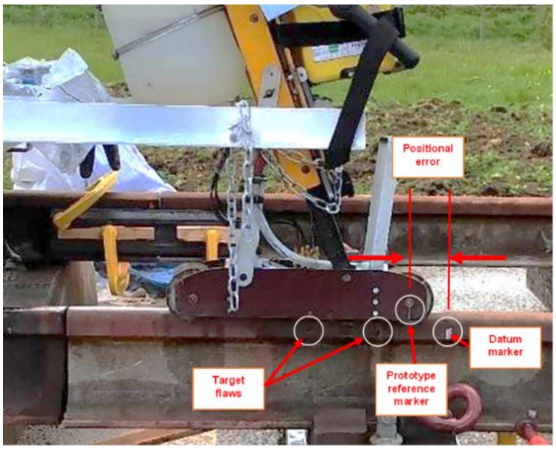

Fig. 8. Prototype positional error measurement.

3. Results and discussion

3.1. Ultrasonics flaw detection

The inspection prototype autonomously detected the two simulated defects in all three tests. With each detection, an audio alert was triggered to notify the operator of the detection. The flaw detector's screen is shown in Figure 9.

The extremely high detection rate was attributable to the relatively small number of tests, as well as the large size and shallow depth of the simulated flaws, which measured 8 mm in diameter and 23 and 27 mm in depth from the railhead's top, respectively. However, the research experiments were not designed to verify the sensitivity of the UT inspection, as this is already a proven technique. It aimed instead at demonstrating the feasibility of autonomous ultrasonic inspections.

Communication with the base was also successful. The prototype autonomously sent the message to the command and control server when a flaw was detected. Figure 10 depicts a tablet screen that received a defect detection message from the Arduino microcontroller.

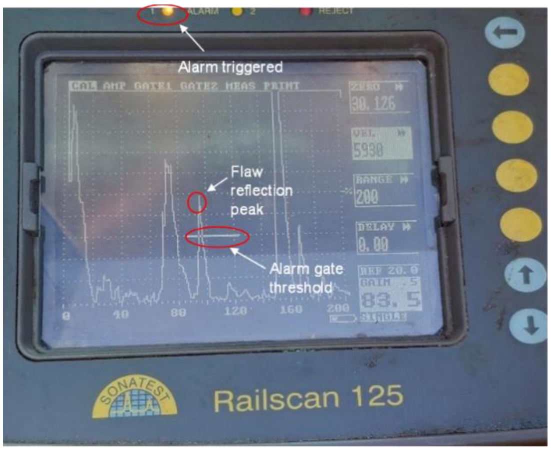

Fig. 9. Flaw detector indicating detection.

3.2. Prototype positional precision assessment

After each test, the actual return position of the prototype was measured using RTK-enhanced GNSS, odometry, and measurements from the test rail and prototype-mounted markers. It was observed that the vehicle did not always return to its starting points exactly. This is attributed to a combination of factors, including GNSS uncertainties, slipping between the vehicle wheels and trolley rollers, skidding, the prototype dynamic response and mechanical backlash.

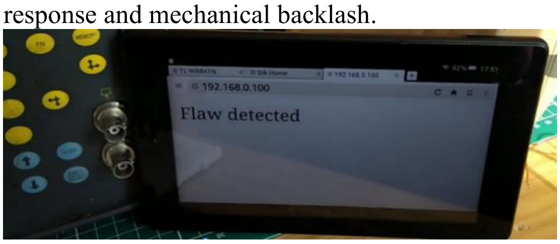

Fig. 10. Simulated flaw detection message to the base.

3.2.1. GNSS results

Figure 11 illustrates the path associated with each test, with each colour representing a separate test. As many as eight satellites were accessible during the testing. Over 1200 samples were collected for every 5 m back and forth displacement, with an estimated error of 25 cm, which was not meet expectations. Additional GNSS analysis and comparison with the prototype at standby yielded an error of comparable magnitude. The measured GNSS resolution uncertainty was therefore deemed systematic due to the poor performance of RTK. The possible reason for it was the loss of satellite signals during tests.

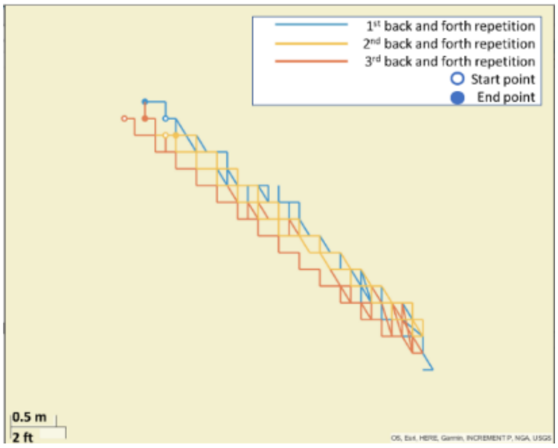

Fig. 11. GNSS path illustration for each conducted test.

3.2.2. Odometry results

Table 4 displays the odometry output value for each test's prototype displacement distance. As observed, the longitudinal error varied roughly between 5 and 7 cm for each forward-reverse movement. It was noted that all measurements "drifted" on the backward displacement. The positional error measured was less than 3 cm at the beginning of each test. Overall, it was more accurate than GNSS during these tests.

The source of errors affecting odometry is attributed to the dynamic response of the unmanned ground vehicle/trolley assembly, which results in uneven contact of the wheels/rollers during the prototype movement.

Table 1. Odometry results.

Test No.	Displacement		Error (cm)	
	Forward	Backward	Longitudinal	Positional
1	5.1816	5.2337	5.21	1.82
2	5.1998	5.2693	6.95	2.94
3	5.1704	5.2211	5.07	1.12

3.2.3. Odometry results

In accordance with the measurements of the markers, the longitudinal error for the three tests conducted was 4 cm for test 1, 6 cm for test 2 and 6 cm for test 3.

These results correlated well with the odometry system and therefore validated the odometry's positional accuracy.

4. Conclusions

This research built, calibrated and tested an autonomous ultrasonic rail inspection prototype consisting of commercially available ultrasonics instrumentation and an unmanned vehicle platform. Consistent fault inspection functionality has been successfully implemented on a section of the test track on TRL 5.

The prototype was able to successfully detect 8mm-diameter artificial rail flaws at depths of 23 and 27 mm in all three repeated tests. Ultrasonic signals above the threshold for flaw detector gate 1 triggered an auditory warning that indicated the detection. Meanwhile, with the integration of autonomy architecture, the prototype delivered a simple plain text message over LAN Wi-Fi to a receiving PC.

The positioning consistency of the inspection prototype was validated using odometry, GPS, and positional measurements relative to the start and finish positions of the vehicle prior to the defect. There was substantial concordance between the results of the three measurement methods. The positional error ranged from 3 to 25 cm, with GPS readings producing the highest error.

However, the current research still has its limitations. Architectural integration and communication of the different systems platforms and components were only achieved at a higher level. It resulted in asynchronous positional information from different navigational and positional systems. The positional information derived from odometry and GNSS refers to the UGV and does not account for the probe offset, and the detected defects information is also not tagged by GNSS. The researchers are still working on the integration and communications between the subsystems and low-level components to improve this deficiency.

The inspection platform's autonomy capabilities are currently still under development. The Warthog vehicle was navigated utilising ordinary GPS+RTK technology, but its current performance was below expectations. Sensor-fusion-based simultaneous localisation and mapping (SLAM) algorithms will appear to provide higher precision.

The detection sensitivity of the prototype was not comprehensively evaluated. Despite simple tests being undertaken to demonstrate the principles of autonomous inspection, these tests only detected the artificially seeded flaws of a specified size, orientation and type. A wider variety of flaws must be invstigated to evaluate the system's sensitivity. The defects were also neither sized nor geolocated. Therefore, further study will conduct tests, inspecting various defects in different sizes, shapes, and depths, representing current critical rail defects.

There are also deficiencies in the mechanical design of the entire prototype system. Skidding, backlash, inertia, and vibration contributed to the prototype's dynamic errors. This was due to the lack of integration of the prototype's fundamental components. The UT system, the unmanned ground vehicle and the RRV trolley were assembled for the first time in the research. The UT system was modified from a manual mode designed for pedestrian examination; therefore, its connection with the prototype was inadequate. These assembly reasons also led to the tests being only performed at a low speed of 0.5 m/s (UGV speed) to avoid skidding and slipping effects. A new UT inspection system designed for on-track testing and a new drive unit would be helpful for smooth rail motion at faster speeds.

Acknowledgements

This project has received funding from the Shift2Rail Joint Undertaking (JU) under grant agreement No 826255. The JU receives support from the European Union's Horizon 2020 research and innovation programme and the Shift2Rail JU members other than the Union."

References

[1] G. Smith, F. Neziri, and A. Sandalli, "Rail Factsheet 2021," London, 2022. [Online]. Available: https://assets.publishing.service.gov.uk/government/uploads/system/uploads/attachment_data/file/1049929/rail-factsheet-2021.pdf

[2] M. P. Papaelias, C. Roberts, and C. L. Davis, "A review on non-destructive evaluation of rails: State-of-the-art and future development," *Proc Inst Mech Eng F J Rail Rapid Transit*, vol. 222, no. 4, pp. 367–384, 2008, doi: 10.1243/09544097JRRT209.

[3] M. Rahman, H. Liu, I. D. Cardenas, A. Starr, A. Hall, and R. Anderson, "Towards an Autonomous RIRS: Design, Structure Investigation and Framework," in *2021 7th International Conference on Mechatronics and Robotics Engineering, ICMRE 2021*, 2021, pp. 164–168. doi: 10.1109/ICMRE51691.2021.9384846.

[4] A. Williams and P. Scharre, Eds., *Autonomous Systems Issues for Defence Policymakers*, vol. 27. NATO Allied Command Transformation, 2015. Accessed: Sep. 29, 2022. [Online]. Available: https://www.researchgate.net/publication/282338125_Autonomous_Systems_Issues_for_Defence_Policymakers

[5] G. Chowdhary, C. Soman, and K. Driggs-Campbell, "Levels of Autonomy for Field Robots — EarthSense." https://www.earthsense.co/news/2020/7/24/levels-of-autonomy-for-field-robots (accessed Sep. 29, 2022).

[6] R. Bostelman and E. Messina, "A-UGV Capabilities Recommended Guide to Autonomy Levels," 2022. Accessed: Sep. 29, 2022. [Online]. Available: https://tsapps.nist.gov/publication/get_pdf.cfm?pub_id=927167

[7] M. Banić, A. Miltenović, M. Pavlović, and I. Ćirić, "Intelligent machine vision based railway infrastructure inspection and monitoring using UAV," *Facta Universitatis, Series: Mechanical Engineering*, vol. 17, no. 3, pp. 357–364, Dec. 2019, doi: 10.22190/FUME190507041B.

[8] Y. Guo, X. Li, L. Jia, and Y. Qin, "An Efficient Rail Recognition Scheme Used for Piloting Mini Autonomous UAV in Railway Inspection," *Proceedings of 2020 International Conference on Sensing, Diagnostics, Prognostics, and Control, SDPC 2020*, pp. 284–290, Aug. 2020, doi: 10.1109/SDPC49476.2020.9353162.

[9] E. Guclu, I. Aydin, and E. Akin, "Development of Vision-Based Autonomous UAV for Railway Tracking," *2021 International Conference on Innovation and Intelligence for Informatics, Computing, and Technologies, 3ICT 2021*, pp. 120–125, Sep. 2021, doi: 10.1109/3ICT53449.2021.9581919.

[10] M. Bobbe, Y. Khedar, J. Backhaus, M. Gerke, Y. Ghassoun, and F. Ploger, "Reactive Mission Planning for UAV based crane rail inspection in an automated Container Terminal," *2020 International Conference on Unmanned Aircraft Systems, ICUAS 2020*, pp. 1286–1293, Sep. 2020, doi: 10.1109/ICUAS48674.2020.9213854.

[11] I. Aydin, M. Sevi, K. Sahbaz, and M. Karakose, "Detection of Rail Defects with Deep Learning Controlled Autonomous UAV," *2021 International Conference on Data Analytics for Business and Industry, ICDABI 2021*, pp. 500–504, 2021, doi: 10.1109/ICDABI53623.2021.9655796.

[12] C. Anderson *et al.*, "Autonomous Inspection System for Railroads," Apr. 2021. doi: 10.1109/SIEDS52267.2021.9483733.

[13] K. Chittal, M. Nandhini, V. Krithika, I. N. Siyo, J. Adithyan, and M. Gowtham, "Autonomous rail inspection," in *IEEE International Conference on Power, Control, Signals and Instrumentation Engineering, ICPCSI 2017*, 2018, pp. 2573–2577. doi: 10.1109/ICPCSI.2017.8392182.